Journal of Catalysis **202,** 354–366 (2001)
doi:10.1006/jcat.2001.3303, available online at http://www.idealibrary.com on IDEAL®

Copper Oxide–Platinum/Alumina Catalysts for Volatile Organic Compound and Carbon Monoxide Oxidation: Synergetic Effect of Cerium and Lanthanum

M. Ferrandon,*,[1] B. Ferrand,* E. Björnbom,* F. Klingstedt,† A. Kalantar Neyestanaki,† H. Karhu,†,‡ and I. J. Väyrynen‡

*Division of Chemical Reaction Engineering, Department of Chemical Engineering and Technology, Royal Institute of Technology, SE-10044 Stockholm, Sweden; †Laboratory of Industrial Chemistry, Process Chemistry Group, Åbo Akademi University, FIN-20500 Åbo, Finland; and ‡Department of Applied Physics, University of Turku, FIN-20014, Turku, Finland

Received March 13, 2001; revised May 22, 2001; accepted June 11, 2001

γ-Alumina alone or modified with 3 mol% additive (La, Ce, or a mixture of both), on which Pt (0.5 mol%), copper oxide (10 mol% Cu), and CuO–Pt were supported, was characterized and tested for the oxidation of a mixture of CO, C_2H_4, and CH_4 in excess oxygen. Catalysts were also subjected to various thermal treatments. Due to its dispersed form, La was more effective than Ce in restraining the formation of corundum and copper aluminate. La–Ce solid solution led to an increase of cerium dispersion and a higher reducibility of ceria. Copper dissolved into the cerium lattice, in CuO/Ce–Al_2O_3, which, after thermal treatments at 1000°C, produced smaller amounts of copper aluminate and lower particle size than on CuO/Al_2O_3. Besides the presence of surface Cu^{2+} species dispersed on alumina, on CuO/Ce–Al_2O_3 temperature-programmed reduction evidenced some Cu^{2+} interacting with ceria. The interaction between Cu and Ce led to stabilization of reduced copper and an enhancement of copper reducibility, thus leading to a substantial increase of CO oxidation for CuO/Ce–Al_2O_3 catalyst. The oxidation ability of Pt for CO and C_2H_4 was improved by the presence of CuO due to an increase of the Pt dispersion and decrease of the Pt particle size. For the oxidation of CH_4 the activities of CuO and CuO–Pt were similar and superior to that of Pt, with or without additives. The presence of Ce decreased the oxidation activity of the CuO–Pt catalyst due to oxidation of Pt. However, a synergetic effect between La and Ce in the CuO–Pt/LaCe–Al_2O_3 catalyst led to more reduced Pt metal and ceria and a well-dispersed Pt with smaller particle size. This resulted in a highly active and thermally stable CuO–Pt/La–Ce–Al_2O_3 catalyst for oxidation reactions of model reactants.

Key Words: **copper oxides; platinum; lanthanum; cerium; carbon monoxide; ethylene; methane; oxidation; stabilization.**

INTRODUCTION

Carbon monoxide, volatile organic compounds, and polyaromatics are ubiquitous air pollutants that give rise to deleterious health and environmental effects. Such compounds are emitted by the combustion of biomass, particularly from small-scale home-heating appliances. The combustion of biomass, especially wood, has recently gained interest in Europe as an advantageous alternative to the utilization of fossil fuels. However, recent and more stringent environmental regulations in Europe have raised concerns over the emissions of CO from biomass fueling, and this has in turn led to incentives for the development of oxidation catalysts to remove pollutants. The applications of such catalysts may also be extended to a host of other air-cleaning processes such as the removal of CO and hydrocarbons, as well as the oxidation of exhaust gas emitted by automobiles.

Several properties are of important consideration when developing total oxidation catalysts, including a low light off, low cost, and high resistance to deactivation. In the initial stage of a wood-burning cycle, as much as 60% of the total emissions can be released, within the first minutes of which the flue gas is led away through a bypass and hence the catalyst is missing when it is needed the most. Low-temperature activity catalysts constitute one of the most promising ways to minimize the cold-start period. Moreover, the catalyst could be placed in a position where maximum peak temperatures are avoided. Ceria is well known to decrease the low-temperature oxidation ability of catalysts due to its numerous properties such as being an oxygen storage compound, promoting the water–gas shift reaction, enhancing the dispersion of metals, and stabilizing the alumina washcoat (1). Ceria is already used in three-way catalysts (2) and combustion catalysts (3). Trovarelli (4) reviewed studies on the different catalytic applications of cerium. Recently, attention has been focused on the utilization of metal oxides, particularly copper oxide, as a substitute for expensive noble metal catalysts (5, 6). Copper catalysts supported on CeO_2/Al_2O_3 are particularly effective for oxidation of CO and CH_4 (5–7) compared to any other base metal catalysts found in

[1] To whom correspondence should be addressed. Fax: 46 (0) 8 10 85 79. E-mail: mafe@ket.kth.se.

0021-9517/01 $35.00

the literature and to a 0.5 wt% Pt catalyst (8). In addition to an enhanced activity, the $CuO/Ce(La)O_2/Al_2O_3$ catalyst also showed a much better resistance to water vapor than other copper catalysts (5, 7, 8). Catalytic activity of metal oxides can be boosted by the addition of very low amounts of noble metals. Previous studies have shown that catalysts based on metal oxides and small amounts of noble metals have a higher resistance to thermal or sulfur dioxide treatments than single component catalysts (6, 9). The thermal stability can be further increased by doping the alumina washcoat with lanthanum (10, 11).

Extensive studies report the effect of cerium on noble metal catalysts, especially in rich- or stoichiometric-fuel conditions, while a few concern the promotion of cerium in metal oxide catalysts and almost none deal with the combination of metal oxide and noble metals.

The purpose of this work is to study the oxidation ability and the thermal stability of a metal oxide (CuO), a noble metal (Pt), or a mixture of both (CuO–Pt) promoted with La, Ce, or a La–Ce mixture in the alumina washcoat. Characterization techniques such as Brunauer–Emmett–Teller (BET), X-ray diffraction (XRD), scanning electron microscopy (SEM), temperature-programmed reduction (TPR), temperature-programmed oxidation (TPO), and X-ray photoelectron spectroscopy (XPS) were used to determine the chemical and physical changes of the samples in the absence or presence of these additives. Catalytic activity was evaluated by oxidation of a mixture of CO, ethylene, and methane in the presence of O_2, CO_2, steam, and N_2.

EXPERIMENTAL

Preparation of Catalysts

γ-Alumina (Puralox SCFa-200, Condea Chemie, Germany, 210 m^2/g) was used as starting material. The addition of 3 mol% lanthanum, 3 mol% cerium, or a mixture of 1.5 mol% lanthanum and 1.5 mol% cerium onto the alumina was done by specific adsorption of a $Me(EDTA)^-$ (Me = La, Ce) complex on alumina (12). This method was originally applied for the deposition of lanthanum. The amounts of lanthanum and cerium were checked by ICP-AES + ICP-QMS.

The active components consisted of CuO alone, platinum alone, or a mixture of CuO and platinum and were deposited on alumina using the deposition-precipitation method (13). Copper nitrate ($Cu(NO_3)_2 \cdot 3H_2O$, Merck, 99.5%) and urea (Merck, pro analysis) were added to a suspension of γ-alumina alone or modified. Platinum salt ($Pt(NO_3)_2$, ChemPur, Germany) was also added to this suspension for the preparation of Pt and CuO–Pt catalysts. The suspension was stirred for several hours at 90°C under inert atmosphere until the formation of a gel. Finally, the slurry was dried overnight at 200°C. The target loadings were 10 mol% Cu and 0.5 mol% Pt of the washcoat counted as Al_2O_3.

Monoliths made of cordierite with a cylindrical shape (diameter: 20 mm, height: 25 mm) and a cell density of 400 cpsi were used. To obtain suitable slurries for dip-coating the monoliths, the impregnated washcoat powders were dispersed in water and ball-milled overnight. The monoliths were then immersed in the slurry for approximately 5 min. The excess slurry was removed by blowing air through the channels. Several dips, followed by drying at 200°C for a few hours, were needed to obtain the desired washcoat loading of ca. 20 wt% of the total catalyst weight. Catalyst denotations are used in the text; for example, $CuO–Pt/La–Ce–Al_2O_3$ catalyst was denoted CuPtLaCeAl.

Thermal Treatments

Several thermal treatments were performed on washcoat powders at various temperatures (800, 900, and 1000°C) and durations (4, 20, 50, 100, and 200 h). Monolithic catalysts were subjected to 800 and 900°C for 4 h in air. The choice of these treatments was motivated by the high temperatures which can be reached in a flue duct of a wood boiler.

Characterization

The surface areas of the catalysts were determined by nitrogen adsorption using a Micromeritics ASAP 2000, after outgassing the samples in vacuum at 250°C.

The phase compositions of the samples were investigated by powder XRD using a Siemens Diffractometer 5000 operating with the following parameters: CuKα radiation of 30 mA, 40 kV, Ni filter, 2θ scanning range of 20–80°, and a scan step size of 0.02. The weight percent of α-Al_2O_3 was determined by comparison of the absolute α-Al_2O_3 intensity of the samples with that of known mixtures of γ-Al_2O_3 and α-Al_2O_3.

The rough-scale distribution of lanthanum was assessed by SEM, using a Zeiss DSM 940 with a resolution of 20–50 Å, combined with energy dispersive X-rays.

TPR was carried out in a continuous flow reactor under 5% H_2 in Ar (up to 700°C, 5°C/min) in a Micromeritics 2900 instrument, equipped with a thermal conductivity detector. The gas flow for TPR experiments was 5 ml/min. The amount of the samples was 200 mg ± 2 mg. The water produced was removed using a cold trap filled with a mixture of liquid nitrogen and 2-propanol (ca. −80°C). Calibration for the hydrogen consumption was carried out by the reduction of CuO.

TPO was carried out in a continuous flow reactor under 5% O_2 in N_2 (up to 800°C, 10°C/min). The flow for TPO experiments was 42 ml/min. Prior to the TPO experiments, the samples were reduced *in situ* in hydrogen flow at 550°C (10°C/min) for 2 h. The samples were then cooled to room temperature and flushed with N_2 for 1 h before start of the TPO analysis. The gases used were of high purity and the

concentrations were determined by quadruple mass spectrometer (Carlo Erba Instruments).

XPS, employing a Perkin-Elmer 5400 instrument using a magnesium anode (200 W), was used to determine the distribution of the elements (2-nm depth). Sensitivity factors used for the quantitative analysis were Al 2p 0.234, La 3d 9.122, Ce 3d 8.808, and Cu 2p 5.321. The binding energies for all the samples were referenced to the C1s line at 284.6 eV and also to the Al 2p peak at 74.4 eV. Both peaks of doublets were included in the peak-fitting procedure. Shirley background has been used unless otherwise stated. Long XPS runs were necessary due to small concentrations, but no significant changes due to reduced species were seen in copper lines (14). A pass energy of 35 eV was used, with typically 2×10^{-8} Torr pressure during the analysis.

Activity Measurements

The activities of the catalysts were studied after different calcination treatments (800 or 900°C for 4 h) for oxidation of a mixture of carbon monoxide (2500 ppm), ethylene (50 ppm), and methane (200 ppm) in the presence of steam (12%), carbon dioxide (12%), oxygen (10%), and nitrogen (balance). Ethylene was included because it is a carcinogenic compound from the combustion of wood and it constitutes a non-negligible amount of the emissions from wood combustion. Methane is a potent greenhouse gas and is a constituent of flue gases from the combustion of wood. The catalysts were tested in a continuous flow tube reactor, made of Inconel steel, which was placed in a tubular furnace. During the activity tests, the temperature of the furnace was increased linearly (3°C/min) from 100 to 800°C. The total flow of the gas mixture was 2.5 L/min, corresponding to a space velocity of approximately 20,000 h^{-1}, which simulates that of wood boilers. The flue gases were analyzed continuously, every 24 s, for C_2H_4 and CH_4 using a gas chromatograph, HP5890, equipped with a flame ionization detector. Carbon monoxide was analyzed by a nondispersive infrared spectrophotometer (NDIR, Rosemount, BINOS 100).

RESULTS

BET Areas

The addition of La and particularly Ce into the alumina washcoat slightly decreased the surface area after calcination up to 1000°C for 4 h compared to that of alumina alone (Table 1). This small decrease is frequently produced by doping with lanthanide oxides of high specific weight and nonporous structure. However, after a longer calcination time, stabilization of the alumina washcoat by La was obtained. The detrimental effect observed with the addition of Ce was retarded in the presence of La, and the surface area of the LaCeAl was still higher than that of alumina alone, after calcination at 1000°C for 200 h.

The presence of active phases had a negative effect on the surface area of the alumina, as seen in Table 2, probably due to the acceleration of alumina phase transformation in the presence of metals (10). Pt samples showed higher surface areas compared to Cu and CuPt samples, certainly due to the larger amount of active phases in the Cu-containing washcoats. In contrast to the samples without active phases, the stabilization effect of the modifiers, particularly La, in the Pt, Cu, and CuPt samples could be seen at a lower calcination temperature (i.e., 900°C).

TABLE 1

BET Surface Area (m^2/g) of Al_2O_3 Alone and Modified after Calcination in Air at 800, 900, and 1000°C (4 and 200 h)

	800°C		900°C		1000°C	
	4 h	200 h	4 h	200 h	4 h	200 h
Al_2O_3	184	148	155	119	144	75
LaAl	176	138	148	117	141	96
CeAl	169	133	138	105	117	37
LaCeAl	174	138	147	116	131	86

Note. La: 3, Ce: 3, La–Ce: 1.5–1.5 mol%/Al_2O_3.

XRD

Table 3 shows the crystalline phases observed in the washcoats after temperature treatments at 900 and 1000°C for 4 and 200 h.

LaAl did not present any corundum (α-Al_2O_3), which showed that La was very effective in retarding the phase transformation. The amount of corundum was highest in the CeAl, which indicated that Ce had a detrimental effect on the alumina phase stabilization.

Despite the fact that, in the LaCeAl sample, the amount of Ce was half of that in CeAl, the intensity corresponding to the CeO_2 peak was much smaller when La is present (Table 3); thus La stabilized CeO_2. Accurate evaluation of

TABLE 2

BET Surface Area (m^2/g) of Pt, Cu, and CuPt Deposited on Al_2O_3 Alone and Modified after Calcination in Air at 800, 900, and 1000°C for 4 h

	800°C	900°C	1000°C
PtAl	173	150	82
PtLaAl	171	159	116
PtCeAl	164	145	102
PtLaCeAl	165	157	113
CuAl	148	94	9
CuLaAl	143	112	57
CuCeAl	144	107	9
CuLaCeAl	140	108	46
CuPtAl	147	87	6
CuPtLaAl	139	110	52
CuPtCeAl	132	90	7
CuPtLaCeAl	131	90	28

Note. La: 3, Ce: 3, La–Ce: 1.5–1.5 mol%/Al_2O_3, Pt: 0.5, Cu: 10 mol%/Al_2O_3.

TABLE 3

Crystalline Phases Determined by XRD of Al_2O_3 Alone and Modified after Calcination in Air at 900 and 1000°C (4 and 200 h)

	900°C		1000°C	
	4 h	200 h	4 h	200 h
Al_2O_3	γ, δ, θ	δ, θ	γ, δ, θ	δ, θ, α(12%)
LaAl	γ, δ	γ, δ	γ, δ	δ, θ
CeAl	γ, δ	γ, δ, θ, CeO_2(169)	γ, δ, CeO_2(72)	α(35%), CeO_2(906)
LaCeAl	γ, δ	γ, δ	γ, δ	θ, α(2%), CeO_2(140)

Note. Weight percent of α-Al_2O_3 and peak intensities of CeO_2 crystallites ($2\theta = 28.546$) are indicated in parentheses. La: 3, Ce: 3, La–Ce: 1.5–1.5 mol%/Al_2O_3.

TABLE 4

α-Al_2O_3, CeO_2, and $CuAl_2O_4$ Crystalline Phases Determined by XRD of Cu Deposited on Al_2O_3 Alone and Modified after Calcination in Air at 800, 900, and 1000°C for 4 h

	800°C	900°C	1000°C
CuAl	—	θ, α(12%)	α(82%), $CuAl_2O_4$(1614)
CuLaAl	—	—	α(9%)
CuCeAl	CeO_2(117)	CeO_2(146)	α(55%), CeO_2(991), $CuAl_2O_4$(891)
CuLaCeAl	CeO_2(53)	CeO_2(72)	α(11%), CeO_2(177)

Note. La: 3, Ce: 3, La–Ce: 1.5–1.5 mol%/Al_2O_3, Cu: 10 mol%/Al_2O_3. Weight percent of α-Al_2O_3 and peak intensities of CeO_2 ($2\theta = 28.546$) and $CuAl_2O_4$ ($2\theta = 36.858$) crystallites are indicated in parentheses.

the position of the maximum reflections of CeO_2 ((111), (200), (220), and (311)) in LaCeAl calcined at 1000°C for 200 h by profile-fitting analysis showed a 2θ shift toward lower angles in the range of 0.06–0.18 with respect to the position of the same peaks in CeAl treated at 1000°C for 200 h (Fig. 1). This was probably due to the dissolution of La^{3+} ions in the CeO_2 lattice (3, 15, 16), because the larger size of the La^{3+} ion causes lattice expansion that in turns results in the observed 2θ shift.

Table 4 shows the crystalline phases and the weight percent of corundum, as well as the peak intensities of CeO_2 and $CuAl_2O_4$ crystallites determined in the washcoats impregnated with copper after temperature treatments at 800, 900, and 1000°C for 4 h.

Corundum was detected after a lower calcination temperature in the CuAl sample, i.e., at 900°C for 4 h instead of at 1000°C for 200 h without copper. The sintering of alumina was thus increased by the presence of copper. However, additives, particularly La, were also effective in retarding the formation of corundum after treatment at 900°C.

The position of the reflections of CeO_2 were shifted to the higher angles of 0.08 in the presence of copper compared to the CeAl sample, both calcined at 1000°C for 4 h, indicating

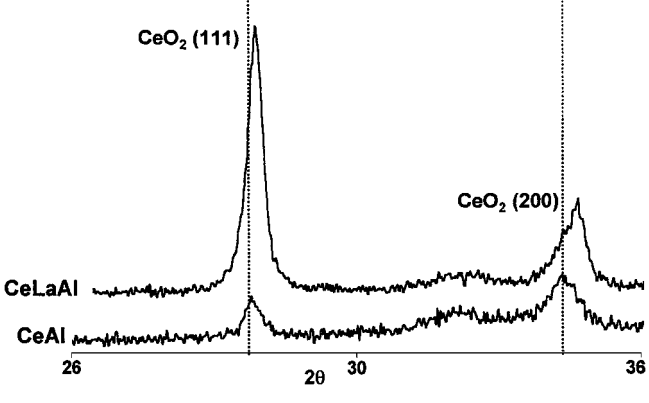

FIG. 1. XRD patterns measured for CeAl and CeLaAl calcined at 1000°C for 200 h in air.

the formation of a Cu–Ce solid solution. Despite the fact that the ionic radius of Cu(II) differs from that of Ce(IV), formation of fluorite-structured cubic solid solution with CuO–CeO_2 systems has also been reported, showing that copper can dissolve within the CeO_2 lattice (17).

No CuO crystallites were observed, probably because of the presence of the "well-dispersed" surface copper species, usually found in copper/alumina with a loading inferior to 8 mol% Cu/100 m^2/g Al_2O_3 (18, 19). In addition, the detection of CuO may be difficult due to overlapping with the corundum diffractogram.

Copper aluminate, $CuAl_2O_4$, was observed after treatment at 1000°C for 4 h in the CuAl and CuCeAl samples. The promotion by Ce of the copper-containing samples produces smaller amounts of $CuAl_2O_4$. In addition, the average particle size of $CuAl_2O_4$ crystallites was 55 and 26 Å, in the CuAl and CuCeAl, respectively, as determined by Scherrer's formula at $2\theta = 36.858°$. Thus, the stabilizing effect of Ce on copper can be ascribed to the interactions between Cu and Ce in the solid solution. No $CuAl_2O_4$ was found in samples containing La (i.e., CuLaCeAl and CuLaAl), indicating an effective inhibition by La of the reaction between copper and alumina.

Pt crystallites were detected in all CuPt samples (Fig. 2), as well as in all Pt catalysts (not shown here), despite the low concentration of Pt loading. No Pt oxides were detected, probably due to their high dispersion and/or their having too small a crystallite size to be made visible by XRD. Pt peak intensities were found to be the highest in the CuPtLaCeAl sample, followed by CuPtAl and CuPtLaAl, and the lowest was in the CuPtCeAl sample. This indicates that the fraction of Pt in metallic form was the highest in CuPtLaCeAl. The fraction of metallic Pt was similar for all four samples of Pt alone and to that of CuPtLaAl.

SEM

SEM analyses coupled with element detection were performed both on alumina samples and on washcoats impregnated with active phases, calcined at 800°C for 4 h. SEM

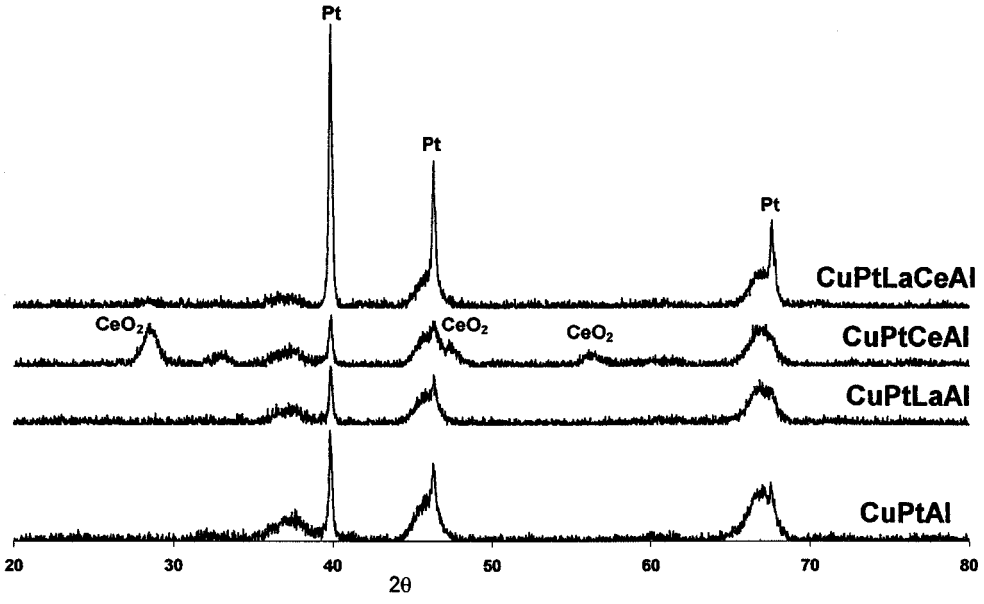

FIG. 2. XRD patterns of CuPt deposited on alumina alone and modified calcined in air at 800°C for 4 h. La: 3, Ce: 3, La–Ce: 1.5–1.5 mol%/Al_2O_3, Pt: 0.5, Cu: 10 mol%/Al_2O_3.

analyses on washcoat samples showed that after calcination at 800°C for 4 h, alumina had a lower particle size when La was present (i.e., 1–5 μm). This was also compared to the alumina doped with Ce (i.e., 1–15 μm; not shown here). Neither Ce nor La could be distinguished from alumina, indicating an effective dispersion.

CuPt and Pt samples were also compared. Backscattered electron detection, based on composition contrast, was used to distinguish the heavy Pt (white spots) from the lighter components in the washcoat. The Pt particle size detected by SEM is rather high due to the limitation of this method. When copper was present, Pt had a better dispersion and a smaller particle size; the maximum particle size was 1.4 μm against 1.0 μm, as seen in Figs. 3a and 3b. Copper oxides may play the role of a new support for Pt, which led to the stabilization of the Pt particles against agglomeration. The presence of La and/or Ce affected the dispersion of Pt onto the washcoat impregnated with copper. La increased the dispersion of Pt (Fig. 3c), whereas Ce hampered it (not shown here). Also, very homogeneous particles of Pt, on the order of 0.4 μm, were obtained when both La and Ce were present in the alumina washcoat (Fig. 3d). It was difficult to distinguish the copper from the Ce probably because of their similar molecular weight or high dispersion.

TPR

Figure 4 shows the TPR profile of only CeAl and LaCeAl calcined at 800°C for 4 h, since those of Al_2O_3 and LaAl did not show any significant hydrogen consumption under 1000°C.

For CeAl and LaCeAl, there were three thermoreduction peaks: a small one at ca. 100°C, a larger one between 200 and 500°C with a maximum of hydrogen consumption at 350°C, and a small one at 600°C. The small peak at 100°C may be attributed to the reduction of a small amount of removable oxygen anions on the bare amorphous alumina

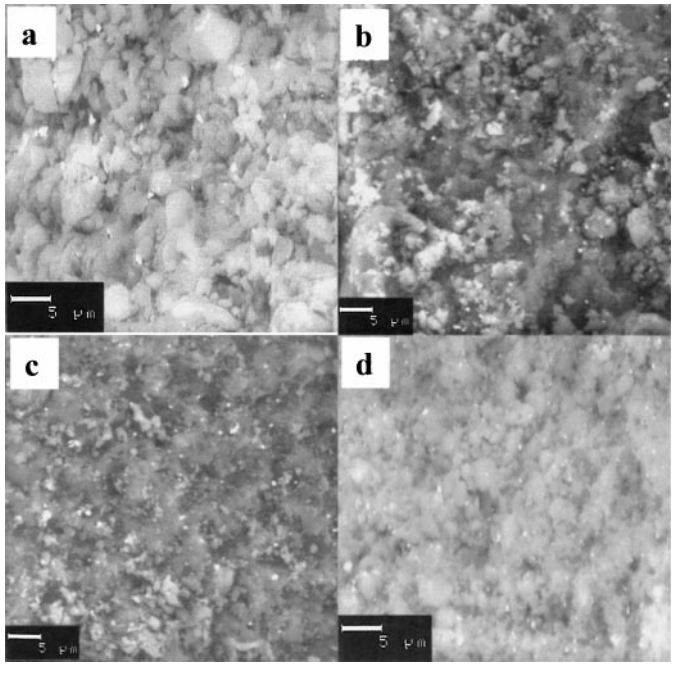

FIG. 3. SEM micrographs of PtAl (a), CuPtAl (b), CuPtLaAl (c), and CuPtLaCeAl (d) calcined in air at 800°C for 4 h. La: 3, La–Ce: 1.5–1.5 mol%/Al_2O_3, Pt: 0.5, Cu: 10 mol%/Al_2O_3.

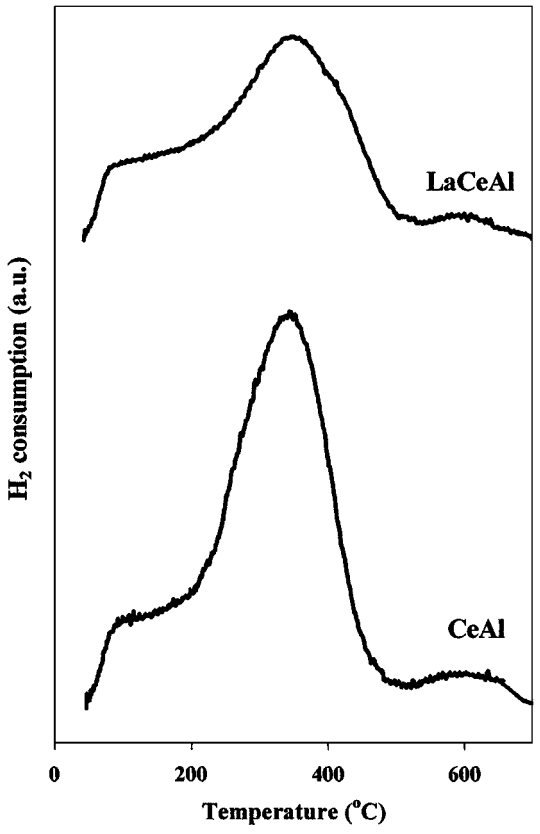

FIG. 4. TPR profiles of CeAl and LaCeAl calcined in air at 800°C for 4 h. Ce: 3, La–Ce: 1.5–1.5 mol%/Al_2O_3. TPR conditions: 5 ml/min, 5% H_2 in Ar.

support in the presence of Ce (20). According to Yao and Yu Yao (20), this peak diminishes when the Ce concentration increases. The second peak corresponds to the reduction of surface-capping oxygen anions attached to a surface Ce^{4+} ion in octahedral coordination (21). The presence of a peak at 600°C may correspond to the reduction of a partially reduced $CeAlO_3$ precursor to $CeAlO_3$ (23). The reaction between CeO_2 and Al_2O_3 to form $CeAlO_3$ normally requires a high-temperature reducing environment (23). However, for well-dispersed and small particles of Ce species supported on Al_2O_3, a significant fraction of Ce^{3+}, which can correspond to $CeAlO_3$ precursor, may be formed during the preparation (23, 24). The absence of a peak corresponding to the reduction of bulk oxygen anions indicates that cerium species are present in the dispersed phase.

The total amount of oxygen removed in the course of TPR was equal to 0.32 and 0.46 μmol O_2/μmol CeO_2, for CeAl and LaCeAl, respectively, which was higher than the value for complete reduction from Ce^{4+} to Ce^{3+} (i.e., 0.25). This confirms the reduction of removable oxygen anions on the alumina. Zotin *et al.* (22) warned about the reliability of the measurements of degree of CeO_2 reduction from the TPR experiments, since adsorbed species may invalidate quantitative estimation. The addition of La increased the reducibility of CeO_2/Al_2O_3 by more than 40%. After calcination of CeAl samples at 900° and 1000°C, TPR showed a large consumption of hydrogen between 600° and 1000°C, indicating the formation of bulk CeO_2 (not shown here).

TPR experiments were performed on Cu deposited on Al_2O_3, La–Al_2O_3, Ce–Al_2O_3, and La–Ce–Al_2O_3, calcined at 800°C for 4 h (Fig. 5). By integrating the TPR curves, an H_2 consumption that exceed the amount required for reduction of the CuO present in the CuCeAl and CuLaCeAl samples could be observed. However, when the amount required for reduction of Ce^{4+} to Ce^{3+} was subtracted from this observed amount, a ratio of H_2/Cu equal to 1 was found, which corresponded to the initial presence of Cu^{2+} species. All the profiles showed a single step reduction, except for CuCeAl, which had two thermoreduction peaks (220° and 239°C). Luo *et al.* (25) could detect two reducible CuO species in mixed CuO/CeO_2, of which one corresponded to small particles of CuO interacting with CeO_2. In our case, no CuO crystallites were formed. Therefore we concluded that the first species reduced at lower temperature correspond to Cu^{2+} interacting with CeO_2 and the second one to Cu^{2+} dispersed on alumina. This interaction between Cu^{2+} and CeO_2 indicates that the rate of oxygen supply from these Cu^{2+} species to the surroundings was more rapid than that of Cu^{2+} dispersed on alumina.

TPR experiments were performed on CuPt deposited on Al_2O_3, La–Al_2O_3, Ce–Al_2O_3, and La–Ce–Al_2O_3. All the profiles were similar, with a single step reduction at around 230°–236°C (not shown here). Also, the reduction occurred at a lower temperature than it did without Pt, due to the spillover effect (26), thus indicating interaction between Pt and copper oxide.

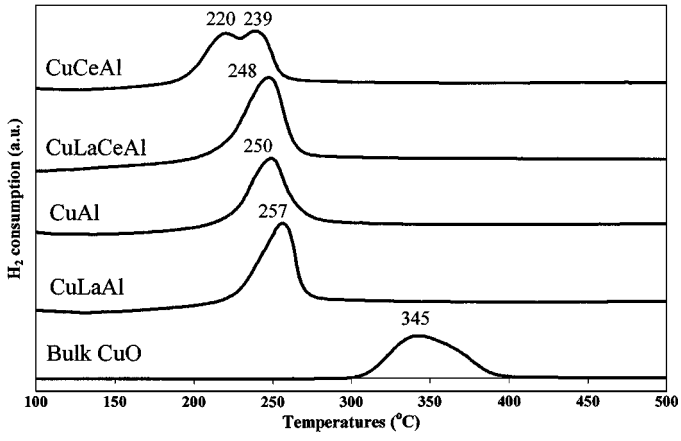

FIG. 5. TPR profiles of CuAl, CuLaAl, CuCeAl, and CuLaCeAl calcined in air at 800°C for 4 h. TPR profile of bulk CuO is added. La: 3, Ce: 3, La–Ce: 1.5–1.5 mol%/Al_2O_3, Cu: 10 mol%/Al_2O_3. TPR conditions: 5 ml/min, 5% H_2 in Ar.

TABLE 5

Data from XPS Analysis of Samples Calcined at 800°C for 4 h in Air[a]

	Binding energy (eV)[b]			%u‴ and v‴ in	Surface atomic ratio		
	La $3d_{5/2}$	Ce $3d_{5/2}$	Cu $2p_{3/2}$	Ce 3d	La/Al	Ce/Al	Cu/Al
LaCeAl	835.9	882.2	—	6	0.012	0.011	—
CuLaCeAl	835.6	883.5	933.6	20	0.010	0.0059	0.060
CuPtAl	—	—	933.6	—	—	—	0.050
CuPtLaAl	835.5	—	933.6	—	0.018	—	0.057
CuPtCeAl	—	882.8	933.6	21	—	0.0059	0.055
CuPtLaCeAl	835.5	882.8	933.6	13	0.0054	0.0054	0.061

[a] La: 3, Ce: 3, La–Ce: 1.5–1.5 mol%/Al_2O_3, Pt: 0.5, Cu: 10 mol%/Al_2O_3.
[b] All binding energies (eV) referenced to C1s = 284.6 eV.

XPS

Table 5 shows the values of the binding energies (BEs) for La $3d_{5/2}$, Ce $3d_{5/2}$, and Cu $2p_{3/2}$, as well as the atomic ratios of La/Al, Ce/Al, and Cu/Al for the LaCeAl, CuLaCeAl, CuPtAl, CuPtLaAl, CuPtCeAl, and CuPtLaCeAl samples, after calcination at 800°C for 4 h.

The La $3d_{5/2}$ BE values for the samples containing La were equal to 835.5 eV, which are substantially higher than the values observed for La_2O_3 (i.e., 833.2–833.8 eV (27–29)), but they are close to the values found for the dispersed "La" phase (i.e., 835.0–836.1 eV (27–30)). This La species gives a La XP line similar to that reported for La_2O_3, $La(OH)_3$, or $LaAlO_3$, which have two doublets (29, 31). However, La_2O_3 or $LaAlO_3$ would be formed at higher concentrations (29, 32). According to Bettman *et al.* (32), under saturation concentration (i.e., 8.5 μmol La/m^2) La is in a two-dimensional lanthanum aluminate (29, 32, 33). Therefore the La, in our samples in the concentration ca. 1.7 and 0.9 μmol La/m^2 in CuPtLaAl and CuPtLaCeAl, respectively, was probably present as a dispersed phase. The atomic ratios of La/Al determined for CuPtLaAl (0.018) and CuPtLaCeAl (0.0054) were close to that of theoretical ratios (i.e., 0.015 and 0.0075, respectively); thus a good dispersion was obtained.

In Fig. 6 peaks u‴ and v‴, u″ and v″, u′ and v′, and u and v correspond to $3d^94f^0$, $3d^94f$, $3d^94f^1$, and $3d^94f^2$ configurations of Ce, respectively. The absence of the u‴ peak in the Ce^{3+} species is interpreted as the lack of the $4f^0$ configuration. According to many authors, v, v″, and v‴ are due to CeO_2, and v′ is primarily due to Ce_2O_3 (23, 30). Five-point fast fourier transform smoothing was applied to spectra before background removal for the $Ce^{3+/4+}$ analysis. Shirley background removal was used in the Ce : Al surface atomic concentration determination, but linear background was yielding better deconvolutions for $Ce^{3+/4+}$ analysis. In the peak-fitting procedure, the Ce $3d_{3/2}$ and Ce $3d_{5/2}$ intensity ratio was 0.66667 and energy separation was 18.1 eV. The relative amounts of Ce^{4+}, as seen in Table 5, were obtained from u‴ and v‴ relative amounts in Ce 3d (23). From Fig. 6, and also Table 5, it can be seen that CuLaCeAl, CuPtLaCeAl, and CuPtCeAl catalysts exhibited higher v, u, v‴, and u‴ concentrations than the LaCeAl sample; thus the first samples described, except the latter, contained primarily CeO_2. When comparing the relative amounts of Ce^{4+} in CuPtLaCe and CuPtCe, it can be observed that the presence of La lowers the Ce^{4+} fraction by 8%, which is in agreement with the results reported by Talo *et al.* (30). Moreover, it can be seen that the presence of Pt on the CuPtLaCeAl sample (when comparing CuLaCeAl and CuPtLaCeAl) also lowers the Ce^{4+} fraction, which suggests the presence of interactions between Pt and CeO_2. The low u‴ peak in LaCeAl suggests that this Ce species on alumina resembles Ce^{3+}, presumably due to dispersed Ce that strongly interacts with alumina. These species could be reduced by TPR;

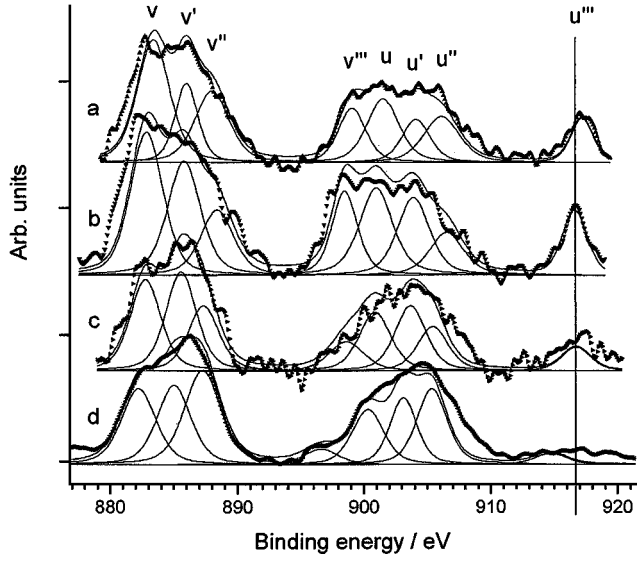

FIG. 6. Ce 3d photoelectron lines deconvoluted. (a) CuLaCeAl, (b) CuPtCeAl, (c) CuPtLaCeAl, and (d) LaCeAl calcined in air at 800°C for 4 h.

thus it cannot be Ce^{3+}, since this is the lowest oxidation state of Ce oxides that can be achieved under experimental conditions (21). Shyu *et al.* (23) refer to this Ce species as the $CeAlO_3$ precursor.

The atomic ratio of Ce/Al for CuPtCeAl (0.0059) was smaller than expected (0.015). According to XRD data, CeO_2 crystallites were already formed at 800°C in the samples containing copper (Table 4), thus resulting in an inhomogeneous dispersion of Ce. However, in CuPtLaCeAl, the Ce/Al ratio (0.0054) was closer to the theoretical value (0.0075). Thus La has increased the dispersion of Ce, which is in agreement with the results from XRD experiments, probably due to the formation of solid solution La–Ce. La has already been reported to enhance the dispersion of CeO_2 (24). The ratio of Ce/Al in LaCeAl is substantially higher than in CuLaCeAl, while the La/Al ratio is similar in both samples. In addition the promotion of copper to LaCeAl increases the fraction of Ce^{4+}; this implies that in CuLaCeAl, the surface CeO_2 has been affected by the deposition of copper, probably because of the formation of a Cu–Ce solid solution as observed by XRD.

The BE of the principal Cu $2p_{3/2}$ peak for the samples was 933.6 eV, which may correspond to the reported values for bulk CuO of ca. 933.6–933.9 eV (19, 34–36). However, the satellite peaks at 963 eV were significantly smaller than that for pure CuO, indicating the presence of another type of Cu^{2+} species, probably a surface spinel (19, 36). Perhaps both CuO and surface Cu^{2+} are present (37). Copper species have similar BEs but different Auger parameters (38). The Cu LMM Auger peaks in CuLaCeAl and CuPtCeAl samples were at 917.5 and 916.4 eV, respectively, indicating that in the CuPtCeAl sample, some Cu^{+} was also detected, whereas in CuLaCeAl primarily Cu^{2+} was found, in agreement with the literature (38–40). The atomic ratio of Cu/Al obtained for CuPtAl was in good agreement with the theoretical ratio (0.050) indicating a very effective dispersion of copper onto alumina.

TPO

The O/Cu ratio for the different Cu and CuPt samples (Table 6) shows a lower reoxidation of copper metal particles after reduction, particularly in the presence of Ce and mixed Ce–La. Since $CeAlO_3$, which may be formed after reduction of the Ce species, is stable to oxidation under oxygen up to 600°C (4), slowness of the oxidation of copper metal to Cu(II) may be due to a higher stability against oxidation of the Cu–Ce solid solution. These interactions resulted in a reoxidation of copper metal only into the Cu(I) state in the presence of Ce, as seen by the O/Cu ratio (Table 6). Fernández-Garcia *et al.* (37) reported a similar result. It seems that the combination of Ce–La resulted in an even higher stability against oxidation of copper. When Pt is present in the samples, oxygen consumption is higher than in its absence, probably due to the potential of Pt to activate oxygen in the gas phase by adsorbing it on the surface and spilling it over the copper metal.

TABLE 6

O/Cu Ratio Determined by TPO Experiment of Cu and CuPt Deposited on Al_2O_3 Alone and Modified after Calcination at 800°C for 4 h in Air

	O/Cu
CuAl	1.00
CuLa	0.78
CuCeAl	0.47
CuLaCeAl	0.08
CuPtAl	1.00
CuPtLaAl	0.94
CuPtCeAl	0.73
CuPtLaCeAl	0.41

Note. La: 3, Ce: 3, La–Ce: 1.5–1.5 mol%/Al_2O_3, Pt: 0.5, Cu: 10 mol%/Al_2O_3.

Activity Measurements on Catalysts Calcined at 800°C for 4 h

Effect of additives on Pt catalysts. Table 7 indicates the temperature for 50% conversion of CO, C_2H_4, and CH_4. The addition of promoters on catalysts with Pt alone had a slight detrimental effect on the oxidation of all the combustibles studied.

Effect of additives on CuO catalysts. For the oxidation of CO, the order of activity was CuCeAl > CuLaCeAl > CuAl > CuLaAl (Fig. 7 and Table 7). For the oxidation of C_2H_4 and CH_4, there was no significant change

TABLE 7

Temperature (°C) for 50% Conversion of the Catalysts Calcined in Air at 800 and 900°C for 4 h[a]

	CO			C_2H_4			CH_4		
	800	900	ΔT[b]	800	900	ΔT	800	900	ΔT
PtAl	200	211	11	206	214	8	629	648	19
PtLaAl	212	212	0	212	212	0	627	631	4
PtCeAl	216	216	0	216	217	1	633	640	7
PtLaCeAl	223	223	0	223	223	0	645	650	5
CuAl	327	297	−30	471	482	11	578	637	59
CuLaAl	332	323	−9	471	500	29	584	611	27
CuCeAl	241	265	24	467	490	23	590	630	40
CuLaCeAl	265	291	26	470	509	39	596	615	19
CuPtAl	175	168	−7	182	210	28	576	643	67
CuPtLaAl	173	162	−11	179	181	2	581	605	24
CuPtCeAl	186	168	−18	190	180	−10	600	633	33
CuPtLaCeAl	156	140	−16	146	167	21	573	624	51

[a] La: 3, Ce: 3, La–Ce: 1.5–1.5 mol%/Al_2O_3, Pt: 0.5, Cu: 10 mol%/Al_2O_3. Mixture—CO: 2500 ppm, C_2H_4: 50 ppm, CH_4: 200 ppm, O_2: 10%, CO_2: 12%, H_2O: 12%, and N_2: 66%.

[b] $\Delta T = T(900) - T(800)$.

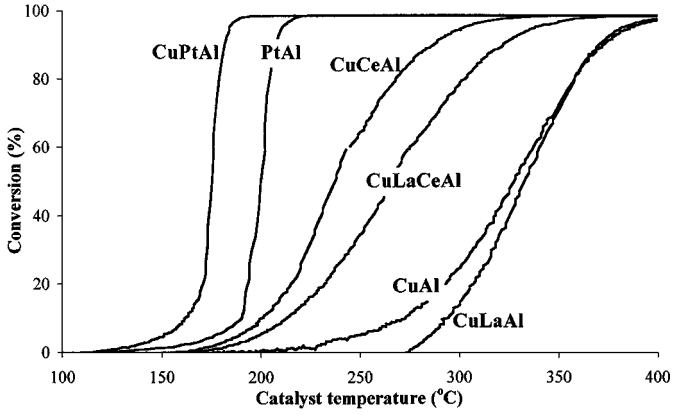

FIG. 7. CO conversion on PtAl, CuPt, and Cu catalysts deposited on alumina alone and modified after calcination in air at 800°C for 4 h. La: 3, Ce: 3, La–Ce: 1.5–1.5 mol%/Al_2O_3, Pt: 0.5, Cu: 10 mol%/Al_2O_3. Mixture—CO: 2500 ppm, C_2H_4: 50 ppm, CH_4: 200 ppm, O_2: 10%, CO_2: 12%, H_2O: 12%, and N_2: 66%.

in activity among the four Cu catalysts. The slight difference seen may be due to the lower surface area of the Cu catalysts with additives, which showed a more pronounced effect on the oxidation of CH_4. It should be noted that although CeO_2 alone has been reported to have some activity for oxidation reactions, it cannot compete with metal oxides such as CuO (4, 25).

The discrepancy between the different behaviors of C_2H_4 and CH_4 with that of CO may be due to the water–gas shift reaction ($CO + H_2O$), which is reported to increase in the presence of CeO_2. To check this effect, an activity measurement on CuCeAl was conducted without any steam, but with steam replaced by N_2 in the feed stream. The CO activities over CuCeAl catalyst are similar with and without steam. Thus, the peculiar performance of CuCeAl for the oxidation of CO cannot be attributed to the shift reaction but to different reaction mechanisms. This is also interesting from the perspective that CuCeAl is insensitive to 12% steam in the feed. The slow step of alkane oxidation has been postulated to be the dissociative chemisorption of the alkane on the metal with the breakage of the weakest C–H bond (41). Absence of a Ce promoter effect for the oxidation of CH_4, contrary to CO oxidation, was also reported (42).

All Pt catalysts had a higher activity than the Cu catalysts for the oxidation of CO and C_2H_4, whereas the opposite was observed for the oxidation of CH_4 (Table 7).

Effect of Pt mixed with CuO. For the oxidation of CO and C_2H_4, the order of activity was CuPtAl > PtAl > CuAl (Fig. 7 and Table 7). There was a synergetic effect between Cu and Pt which made the CuPt catalyst more active for the oxidation of CO and C_2H_4 than with the PtAl and CuAl catalysts. One explanation could be the better dispersion and smaller particle size of Pt when copper is present, as observed by SEM. A better dispersion of Pt in the washcoat has been found to enhance the activity for CO oxidation at low CO concentration in air (43).

For the oxidation of CH_4, the order of activity was CuAl ≅ CuPtAl > PtAl. There was no synergetic effect for the oxidation of CH_4 as expected. Namely, the "active phase" for CH_4 oxidation was CuO itself since the activities of the CuAl and CuPtAl catalysts were similar for the oxidation of CH_4 and larger than that of Pt. The difference between the activity of the CuAl and CuPtAl catalysts was probably due to the small difference in surface area.

Similar results were observed for Pt, Cu, and CuPt deposited on the other supports (La–Al_2O_3, Ce–Al_2O_3, and La–Ce–Al_2O_3), except that for the oxidation of CH_4, CuPtLaCeAl had a lower ignition temperature compared to CuLaCeAl. This will be discussed later.

Effect of additives on CuO–Pt catalysts. For the oxidation of CO and C_2H_4 the order of activity was CuPtLaCeAl > CuPtLaAl = CuPtAl > CuPtCeAl (Fig. 8 and Table 7). A 100% conversion of C_2H_4 and CO was reached at 146° and 156°C, respectively, with the CuPtLaCeAl catalyst. According to our XRD results, the share of Pt metal was lowest in CuPtCeAl, indicating that oxidation of Pt was highest in this sample. This could explain the low activity of the CuPtCeAl catalyst. The rate of alkane oxidation in excess air has also been reported by some authors to be strongly suppressed by adding CeO_2 to Pt and Pd catalysts (2, 44, 45). Indeed, the metal oxides are believed to be poor catalysts for alkane oxidation, except for CH_4 for which PdO has been reported to be more active (3). Concerning the oxidation of CO, there are some contradictory results in the literature. It was reported that small quantities of Ce (up to 2%) increased the oxidation of CO in the oxidizing environment over fresh Pt catalysts, whereas a higher amount hampered it (46), because CeO_2 promoted the oxidation of

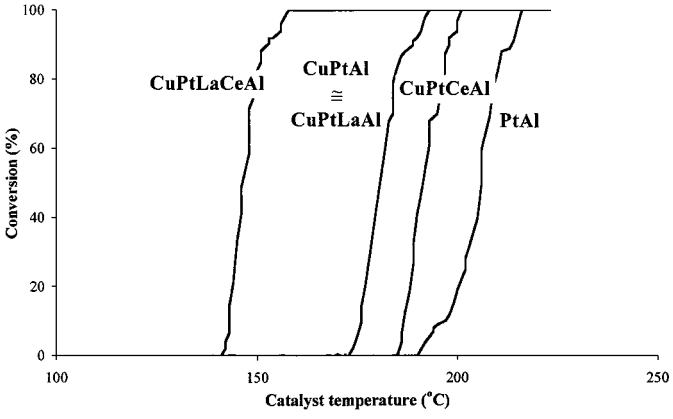

FIG. 8. C_2H_4 conversion over the PtAl catalyst and CuPt catalysts deposited on alumina alone and modified after calcination in air at 800°C for 4 h. La: 3, Ce: 3, La–Ce: 1.5–1.5 mol%/Al_2O_3, Pt: 0.5, Cu: 10 mol%/Al_2O_3. Mixture—CO: 2500 ppm, C_2H_4: 50 ppm, CH_4: 200 ppm, O_2: 10%, CO_2: 12%, H_2O: 12%, and N_2: 66%.

Pt over $Pt/CeO_2/Al_2O_3$. However, there was a synergetic effect between La and Ce since the activity of the CuPt-LaCeAl catalyst for the oxidation of CO and particularly for C_2H_4 was highest. It has been reported that a combination of La and Ce improved the light-off performance of the $Pt/Rh/CeO_2/La_2O_3/Al_2O_3$ catalysts for abatements of CO, NO, and hydrocarbons (16).

For the oxidation of CH_4, there was no significant effect of the promoters (Table 7). The activities of the CuPt catalysts deposited on Al_2O_3 alone, La–Al_2O_3, or La-Ce-Al_2O_3 were quite similar. It seems that the synergetic effect due to the addition of both La and Ce compensated for the loss of surface area of the CuPtLaCeAl catalyst since its activity was similar to that of CuPtAl, which had a slightly higher surface area. The addition of Ce had a negative effect since the activity was lower for the CuPtCeAl catalyst, probably due to its lower surface area.

All the CuPt catalysts had a higher activity than the Pt and Cu catalysts for the oxidation of CO and C_2H_4. Moreover all the CuPt catalysts had almost the same activity as the Cu catalysts for the oxidation of CH_4 but a higher activity compared to the Pt catalysts.

Activity Measurements on Catalysts Calcined at 900°C for 4 h

The calcination temperature at 900°C had a negative effect on the activity of the PtAl catalyst for the oxidation of all the combustibles studied here as seen in Table 7. This may be due to sintering of the Pt particles and decreasing of the surface area of the catalyst. The addition of additives, particularly La, had a stabilizing effect on the oxidation, since almost no deactivation was seen for all the Pt catalysts doped with additives.

Among the CuO catalysts calcined at 900°C, the CuCeAl still had the best activity for the oxidation of CO. The slight decrease of activity may be the result of a decrease in oxygen mobility caused by CeO_2 crystallization (47). The activity for CO conversion was increased for the CuAl and CuLaAl catalysts calcined at 900°C compared to those calcined at 800°C, whereas it was hampered for the oxidation of C_2H_4 and more particularly for CH_4. This may be due to an enrichment and growth of CuO at the surface, which have been reported to lead to an increase in CO oxidation and to a decrease in CH_4 oxidation (19). The copper catalysts stabilized by La (CuLaAl and CuLaCeAl) had the best activities for the oxidation of CH_4, due to their higher surface areas compared to that of CuAl.

Concerning the mixed catalysts, the order of catalytic activity was CuPtLaCeAl > CuPtLaAl > CuPtCeAl $\cong$ CuPtAl > PtAl for CO oxidation. There was an increase in CO oxidation after calcination at 900°C for all the CuPtAl catalysts, probably due to a stronger synergetic effect between Cu and Pt. The larger effect was observed when either Ce alone or both Ce and La were added with a decrease of the temperature for 50% conversion of around 20°C. The enhancement in activity can be attributed to an enrichment in Pt that migrated at the surface with a higher calcination temperature and hence the synergetic effects, which were alreay observed for the CuPt samples calcined at 800°C, are emphasized. For the oxidation of C_2H_4, the CuPtLaCeAl catalyst had the best activity among the CuPt catalysts, due to the synergetic effect between Ce and La. Doped catalysts had a higher activity compared to undoped CuPt, probably due to the stabilization effect of the washcoat. For the oxidation of CH_4, the order of activity of the CuPtAl catalysts resembled the order of the BET surface area. The addition of La had a positive effect since the CuPtLaAl and CuPtLaCeAl catalysts had the best activities due to stabilization of the washcoat.

DISCUSSION

Structural Characteristics of the Washcoat—Effect of La or Ce

XPS measurements evidenced the formation of a "surface lanthanum aluminate" phase, and XRD did not detect any La-containing phase on any of samples even after high-temperature treatments up to 1000°C. Ce was also found as a dispersed phase in samples without Cu or Pt when calcined below 900°C, as observed by XRD, TPR, and XPS in the CeAl and LaCeAl samples. This is in agreement with Yao and Yu Yao (20) who conducted TPR and chemisorption studies and Shyu *et al.* (23) who did not observe the formation of CeO_2 bulk below a concentration of Ce of ca. 2.5 μmol CeO_2/m^2 alumina, which is much higher than our values (1.7 μmol CeO_2/m^2 alumina for 3 mol%Ce/Al_2O_3). These well-dispersed Ce species were reported to be $CeAlO_3$ precursors, in agreement with our results from TPR and XPS measurements. Che *et al.* (48) proposed that $CeAlO_3$ precursors were stabilized in the cation vacancies of the alumina surface. However, in the presence of copper, already at 800°C, some CeO_2 crystallites could be detected by XRD and also by XPS, probably due to the sintering of CeO_2 accelerated by the addition of copper. La was a more effective inhibitor to washcoat sintering than Ce, as seen by the results obtained from BET, XRD, and SEM experiments. The superiority of La over Ce on the thermal stabilization of washcoats has also been reported by other researchers (3, 11, 49, 50). Some authors maintained that La is inserted into the crystal lattice of alumina with a spinel structure, while Ce remains on the surface in the form of CeO_2 (3, 11). This characteristic difference explains why the modification by La was more effective than that of Ce for improving the thermal stability of alumina. Also, this higher dispersion of La led to a more efficient restraint of the undesirable reaction between alumina and CuO that forms copper aluminate.

When La was added, a Ce–La solid solution could be detected by XRD. The insertion of La into the CeO_2 lattice resulted into the stabilization of CeO_2, as seen by a lower formation of CeO_2 crystallites (XRD) and an increase of Ce dispersion, as determined by XPS. It has also been reported that La inhibits the sintering of CeO_2 (3). Remarkably, dopants whose radii are larger than that of Ce^{4+} (e.g., La) were reported to significantly stabilize CeO_2 (51). These interactions also promote the reducibility of CeO_2, as seen by a higher H_2 consumption. Since the oxygen storage capacity of CeO_2 is related to its reducibility, La increases the oxygen storage capacity of CeO_2. Similar results have been found in the literature (3, 16, 52). When La^{3+} is partly substituted for Ce^{4+}, the charge is compensated by the formation of oxygen vacancies which promote the diffusion of oxygen in the bulk. This results in a higher oxygen storage capacity in the presence of the dopant.

Cu–Ce Interactions

XRD measurements determined the formation of a solid solution between Ce and Cu. These interactions may be reached during the deposition of copper that preferentially deposited on CeO_2, as observed from transmission electron microscopy studies by Fernández-García *et al.* (37). Namely, in the present work, hydrogen TPR on $CuO/Ce–Al_2O_3$ evidenced the presence of two copper species, of which Cu^{2+} interacting with CeO_2 gets reduced at lower temperature. The surface concentration of Ce was affected by the subsequent deposition of copper, whereas La was not, as seen by a change of the atomic ratios of Ce/Al and a higher fraction of Ce^{4+} in the presence of copper calculated from XPS measurements. Contacts between Cu and Ce resulted in the stabilization of copper, as seen by a lesser formation and a lower average particle size of bulk copper aluminate in CuCeAl compared to CuAl after aging at 1000°C for 4 h. The stabilization of copper by CeO_2 can also be seen by the slower reoxidation and lower oxygen consumption of copper in the presence of CeO_2 during TPO after reduction of the samples up to 700°C. The promotion of CeO_2 into copper catalyst led to a 80°C decrease in temperature for 50% conversion of CO. We showed that this enhancement is seen even without any steam in the feed; thus it cannot be accounted for in the water–gas shift reaction. Some authors (5, 17) reported the creation of anionic vacancies due to the insertion of Cu^{2+} into the CeO_2 lattice. The insertion of copper into the CeO_2 lattice led to the creation of vacancies that increase the copper reducibility (i.e., lower the copper oxide reduction temperature). This enhancement in oxygen mobility in copper catalysts doped with CeO_2 resulted in a higher redox process, according to the Mars–van Krevelen type of mechanism, and significantly promotes the CO oxidation. Luo *et al.* (25) also claimed that the enhancement in CO oxidation was due to CO adsorption that occurs only on Cu interacting with CeO_2. Despite the fact that in this study, BE determined from XPS and H_2 consumption from TPR experiments evidenced the presence of Cu^{2+}, an Auger peak that can be assigned to Cu^+ was also found in CuPtCeAl. The stabilization of reduced copper, as Cu^+, was also clearer after reduction and reoxidation during TPO of CuCeAl. Liu and Flytzani-Stephanopoulos (7) reported that CeO_2 enhanced the oxidation of CO on CuO catalysts. The authors attributed these results to the presence of small, dispersed Cu^+ clusters stabilized by interaction with CeO_2 (39). They proposed a model, where copper clusters provide surface sites for CO adsorption and the CeO_2 provides the oxygen source, which is then transferred to CO. Jernigan and Somorjai (38) indeed compared the CO oxidation over CuO, Cu_2O, and Cu and concluded that the apparant activation energy increases with increasing copper oxidation state. Therefore both effects (from Cu^{2+} interacting with CeO_2 and the presence of Cu^+) may be present in the CuCeAl catalyst.

Despite a 50% lower amount of CeO_2 in CuLaCeAl compared to CuCeAl, the CO oxidation is favored, probably because the presence of La promotes the effect of CeO_2 on copper, as observed by an increase of CeO_2 reducibility with La during TPR experiments. Thus La and Ce do have a synergetic effect on the catalytic oxidation over the copper catalyst.

Synergism between La and Ce on CuO–Pt Catalysts

Characterization studies and activity measurements confirmed the slight influence of the additives (La, Ce, or both of them) on pure Pt catalysts. Markedly, the effect of the additives on Pt catalysts was much clearer when copper was also present. Namely, in CuPt catalysts Ce induced a lower share of metallic Pt whereas mixed La–Ce brought about a higher fraction of metallic Pt and reduced CeO_2, compared to CuPt without additives.

In the present study, CuPtCeAl and PtCeAl catalysts had a lower activity than CuPtAl and PtAl catalysts, respectively. Several authors reported that after pretreatment of Pt/CeO_2-containing catalysts in an oxidizing atmosphere, the Pt at the interface with CeO_2 was partially oxidized, thus leading to worse or similar activity compared to the Pt/alumina catalyst (42, 53).

However, when Ce was mixed with La in the CuPtLaCeAl catalyst, more reduced CeO_2 and Pt was found, as determined by XPS and XRD, respectively, compared to CuPtCeAl catalyst, as well as the formation of $Pt–CeO_2$ interactions. These resulted in a very active CuPtLaCeAl catalyst compared to CuPtAl, CuPtCeAl, or any Pt catalysts. In the literature, Pt/CeO_2–alumina catalysts have been found to have considerable activity for CO oxidation at low temperatures under stoichiometric fuel conditions but the improvement was present only after a high-temperature reduction with H_2 (54) and CO (53). Serre *et al.* (53) proposed that the high temperature was needed to reduce PtO_2 and

PtO at the interface between Pt and CeO_2 and that it was this reduced Pt in contact with CeO_2 that was responsible for the high activity. Reduced CeO_2 in the vicinity of reduced Pt atoms on the surface were also proposed by other authors to be the most active sites of the catalyst, especially for CO oxidation (55). Serre *et al.* (56) gave two interpretations of the Pt–CeO_2 interactions: (i) a C–O bond weakening when CO is adsorbed on Pt particles, and thus a CO adsorbed near the Pt–CeO_2 interface will more easily insert an oxygen atom from CeO_2 into its structure and will quickly desorb as CO_2, and (ii) a decrease of the Ce–O bond strength for CeO_2 localized near Pt.

In this study, the promotion of Pt/CeO_2–alumina catalyst with both Cu and La could improve significantly the oxidation for CO, C_2H_4, and CH_4 in oxidizing atmosphere and without any prior reducing treatment of the samples. This is an advantage since prereducing treatment would have only a short time effect on the activity of the catalysts and hence be useless for total oxidation applications.

CONCLUSIONS

- $CeAlO_3$ precursor was detected on doped alumina. However, CeO_2 crystallites could be observed at 900°C after an aging for 200 h and at 1000°C after 4 h, whereas in the presence of active phases, they were detected already at 800°C for 4 h. For La, a stable surface $LaAlO_3$ was found on doped samples.
- Due to its dispersed form, the La phase contributed to the thermal stabilization of the alumina washcoat to a higher extent than the Ce phase did. Also, in the presence of active phases, La prevented the reaction of alumina with CuO to form the inactive spinel compound at high temperature.
- The formation of a La–Ce solid solution led to the stabilization of CeO_2 and an increase of its dispersion as well as the enhancement of its oxygen mobility.
- Copper dissolved into the CeO_2 lattice, yielding a Cu–Ce solid solution as detected by XRD and TPR, which led to a higher thermal stability of copper by producing smaller amounts of $CuAl_2O_4$ and lower particle size than on CuO/Al_2O_3 after thermal treatment at 1000°C. In addition, CeO_2 promoted the formation of some reduced copper (Cu^+) in catalysts calcined in air, particularly after a redox cycle. Also, this Cu–Ce interaction brought down a significant increase of oxygen mobility that resulted in an increase of copper reducibility. Thus, these last two effects led to a substantial enhancement of CO oxidation.
- The presence of copper, in CuO–Pt/Al_2O_3 catalysts, enhanced the activity for the oxidation of CO and C_2H_4 compared to Pt/Al_2O_3 due to an increase of Pt dispersion and a decrease of its particle size. For the oxidation of CH_4 the activities of CuO/Al_2O_3 and CuO–Pt/Al_2O_3 were similar and superior to that of Pt/Al_2O_3.
- The additives affected slightly the Pt/Al_2O_3 catalysts, while on the CuO–Pt/Al_2O_3 catalysts the addition of Ce decreased the fraction of reduced Pt. This oxidation of Pt into less active Pt oxides in the presence of Ce, in CuO–Pt/Ce–Al_2O_3 catalysts, was counteracted by the addition of La which facilitated the reduction of both Pt and CeO_2, thus enhancing the catalytic activity. Therefore the combined CuO–Pt/La–Ce–Al_2O_3 catalyst was concluded to have the highest activity and thermal stability of all the catalysts tested, making it the best option in this study for the oxidation of CO and volatile organic compounds.

ACKNOWLEDGMENTS

The Swedish National Energy Administration (STEM), the Swedish National Board for Industrial and Technical Development (NUTEK), and the European Commission (the FAIR-program, CT95-0682) are gratefully acknowledged. We thank Inga Groth for help with the SEM at the Division of Chemical Technology, the Royal Institute of Technology.

REFERENCES

1. Harrison, B., Diwell, A. F., and Hallett, C., *Platinum Metals Rev.* **32**(2), 73 (1988).
2. Gandhi, H. S., and Shelef, M., *in* "Catalysis and Automotive Pollution Control" (A. Crucq and A. Frennet, Eds.), Vol. 30, p. 199. Elsevier, Amsterdam, 1987.
3. Groppi, G., Cristiani, C., Lietti, L., Ramella, C., Valentini, M., and Forzatti, P., *Catal. Today* **50**, 399 (1999).
4. Trovarelli, A., *Catal. Rev.—Sci. Eng.* **38**, 439 (1996).
5. Xavier, K. O., Rashid, K. K. A., Sen, B., Yusuff, K. K. M., and Chacko, J., *in* "Recent Advances in Basic and Applied Aspects of Industrial Catalysis" (T. S. R. Prasada Rao and G. Murali Dhar, Eds.), Vol. 113, p. 821. Elsevier, Amsterdam, 1998.
6. Ferrandon, M., Carnö, J., Järås, S., and Björnbom, E., *Appl. Catal. A* **180**, 153 (1999).
7. Liu, W., and Flytzani-Stephanopoulos, M., *J. Catal.* **153**, 304 (1995).
8. Liu, W., and Flytzani-Stephanopoulos, M., *in* "Environmental Catalysis" (G. Centi *et al.*, Eds.), p. 527. SCI Publisher, Rome, 1995.
9. Klingstedt, F., Kalantar Neyestanaki, A., Lindfors, L.-E., Ollonqvist, T., and Väyrynen, J., *React. Kinet. Catal. Lett.* **70**(1), 3 (2000).
10. Burtin, P., Brunelle, J. P., Pijolat, M., and Soustelle, M., *Appl. Catal.* **34**, 225 (1987).
11. Church, J. S., and Cant, N. W., *Appl. Catal.* **101**, 105 (1993).
12. Tijburg, I. I. M., Geus, J. W., and Zandbergen, H. W., *J. Mater. Sci.* **26**, 6479 (1991).
13. Xiaoding, X., Vonk, H., Cybulski, A., and Moulijn, J. A., *in* "Preparation of Catalysts VI" (G. Poncelet, P. Grange, P. A. Jacobs, and B. Delmon, Eds.), p. 1069. Elsevier, Amsterdam, 1995.
14. Wallbank, B., Johnson, C. E., and Main, I. G., *J. Electron Spectrosc.* **4**, 263 (1974).
15. Shannon, R. D., and Prewitt, C. T., *Acta Crystallogr. B* **25**, 925 (1969).
16. Miki, T., Ogawa, T., Haneda, M., Kakuta, N., Ueno, A., Tateishi, S., Matsuura, S., and Sato, M., *J. Phys. Chem.* **94**, 6464 (1990).
17. Lamonier, C., Bennani, A., D'Huysser, A., Aboukaïs, A., and Wrobel, G., *J. Chem. Soc., Faraday Trans.* **92**(1), 131 (1996).
18. Centi, G., Perathoner, S., Biglino, D., and Giamello, E., *J. Catal.* **151**, 75 (1995).
19. Park, P. W., and Ledford, J. S., *Appl. Catal. B* **15**, 221 (1998).
20. Yao, H. C., and Yu Yao, Y.-F., *J. Catal.* **86**, 254 (1984).
21. Rosynek, M. P., *Catal. Rev.—Sci. Eng.* **16**(1), 111 (1977).

22. Zotin, F. M. Z., Tournayan, L., Varloud, J., Perrichon, V., and Fréty, R., *Appl. Catal. A* **98**, 99 (1993).
23. Shyu, J. Z., Weber, W. H., and Gandhi, H. S., *J. Phys. Chem.* **92**, 4964 (1988).
24. Graham, G. W., Schmitz, P. J., Usmen, R. K., and McCabe, R. W., *Catal. Lett.* **17**, 175 (1993).
25. Luo, M.-F., Zhong, Y. J., Yuan, X.-X., and Zheng, X.-M., *Appl. Catal. A* **162**, 121 (1997).
26. Gentry, S. J., Hurst, N. W., and Jones, A., *J. Chem. Soc., Faraday Trans. I* **77**, 603 (1981).
27. Alvero, R., Bernal, A., Carrizosa, I., and Odriozola, J. A., *Inorg. Chim. Acta* **140**, 45 (1987).
28. Ledford, J. S., Houalla, M., Proctor, A., Hercules, D. M., and Petrakis, L., *J. Phys. Chem.* **93**(18), 6770 (1989).
29. Haack, L. P., de Vries, J. E., Otto, K., and Chattha, M. S., *Appl. Catal. A* **82**, 199 (1992).
30. Talo, A., Lahtinen, J., and Hautojärvi, P., *Appl. Catal. B* **5**, 221 (1995).
31. Siegmann, H. C., Schlapbach, L., and Brundle, C. R., *Phys. Rev. Lett.* **40**(14), 972 (1978).
32. Bettman, M., Chase, R. E., Otto, K., and Weber, W. H., *J. Catal.* **117**, 447 (1989).
33. Scheithauer, M., Knözinger, H., and Vannice, M. A., *J. Catal.* **178**, 701 (1998).
34. Wolberg, A., Ogilvie, J. L., and Roth, J. F., *J. Catal.* **19**, 86 (1970).
35. Ertl, G., Hierl, R., Knözinger, H., Thiele, N., and Urbach, H. P., *Appl. Surf. Sci.* **5**, 49 (1980).
36. Strohmeier, B. R., Leyden, D. E., Field, R. S., and Hercules, D. M., *J. Catal.* **94**, 514 (1985).
37. Fernández-García, M., Gómez Rebollo, E., Guerrero Ruiz, A., Conesa, J. C., and Soria, J., *J. Catal.* **172**, 146 (1997).
38. Jernigan, G. G., and Somorjai, G. A., *J. Catal.* **147**, 567 (1994).
39. Liu, W., and Flytzani-Stephanopoulos, M., *J. Catal.* **153**, 317 (1995).
40. Batista, J., Pintar, A., Mandrino, D., Jenko, M., and Martin, V., *Appl. Catal. A* **206**, 113 (2001).
41. Cullis, C. F., Keene, D. E., and Trimm, D. L., *J. Catal.* **19**, 378 (1970).
42. Park, P. W., and Ledford, J. S., *Catal. Lett.* **50**, 41 (1998).
43. Drewsen, A., Ljungqvist, A., Skoglundh, M., and Andersson, B., *Chem. Eng. Sci.* **55**, 4939 (2000).
44. Yu Yao, Y.-F., *Ind. Eng. Chem. Prod. Res. Dev.* **19**, 293 (1980).
45. Shyu, J. Z., Otto, K., Watkins, W. L. H., Graham, G. W., Belitz, R. K., and Gandhi, H. S., *J. Catal.* **114**, 23 (1988).
46. Summers, J. C., and Ausen, S. A., *J. Catal.* **58**, 131 (1979).
47. Funabiki, M., and Yamada, T., SAE Paper 881684.
48. Che, M., Kibblewhite, J. F. J., Tench, A. J., Dufaux, M., and Naccache, C., *J. Chem Soc., Faraday Trans. I* **69**, 857 (1973).
49. Ozawa, M., Kimura, M., and Isogai, A., *J. Mater Sci. Lett.* **9**, 709 (1990).
50. Ahlström-Silversand, A. F., and Odenbrand, C. U. I., *Appl. Catal. A* **153**, 157 (1997).
51. Kubsh, J. E., Rieck, J. S., and Spencer, N. D., *in* "Catalysis and Automotive Pollution Control II" (A. Crucq, Ed.), p. 125. Elsevier, Amsterdam, 1991.
52. Cho, B. K., *J. Catal.* **131**, 74 (1991).
53. Serre, C., Garin, F., Belot, G., and Maire, G., *J. Catal.* **141**, 9 (1993).
54. Diwel, A. F., Rajaram, R. R., Shaw, H. A., and Truex, T. J., *in* "Catalysis and Automotive Pollution Control II" (A. Crucq, Ed.), Vol. 71, p. 139. Elsevier, Amsterdam, 1991.
55. Nunan, J. G., Robota, H. J., Cohn, M. J., and Bradley, S. A., *J. Catal.* **133**, 309 (1992).
56. Serre, C., Garin, F., Belot, G., and Maire, G., *J. Catal.* **141**, 1 (1993).